

A New Ionization Correction Factors for Chemical Composition Determination of the Galactical Planetary Nebulae and the HII Regions in the Blue Compact Dwarf Galaxies

N.V.Havrylova¹,

V.V.Holovaty² and B.Ya.Melekh³

Chair of Astrophysics, Ivan Franco National University of Lviv,

Kyryla and Mefodia str. 8, Lviv 79005, Ukraine

¹e-mail: gavrylova@physics.wups.lviv.ua,

²e-mail: gol@astro.franco.lviv.ua,

³e-mail: melekh@physics.wups.lviv.ua

New analytical expressions for Ionization Correction Factors (ICFs) are obtained from the photoionization models (PhMs) grid separately for the planetary nebulae (PNe) and the HII regions in the Blue Compact Dwarf Galaxies (BCDG). The PhMs grid was calculated using the CLOUDY94 code of Ferland [1]. All the PhMs were spherically symmetric.

The free parameters for PNe grid were the spectral energy distribution (SED) of the PNe nuclei at $\lambda 912\text{\AA}$, chemical composition of the nebular gas taken as averaged values from [2], the nebular gas filling factor (0.1, 0.5 and 1):

The SEDs of the nuclei at $\lambda 912\text{\AA}$ correspond to the stellar atmosphere models of Clegg & Middlemass [3] corrected for the stellar wind presence by using Zanstra relationships $Z(\text{HeII})$ from Gabler, Kudritzki & Mendez [4]. Our correction based on "increasing" or "decreasing" Clegg & Middlemas SEDs at the range $\lambda \leq 228\text{\AA}$ for coincidence of new Zanstra relations with ones from [4]. The stellar atmosphere models from Clegg & Middlemas were approximated at $\lambda \leq 228\text{\AA}$ by a power-law spectra and the number of ionizing quanta was changed in this range without the color temperature changing of the corresponding model.

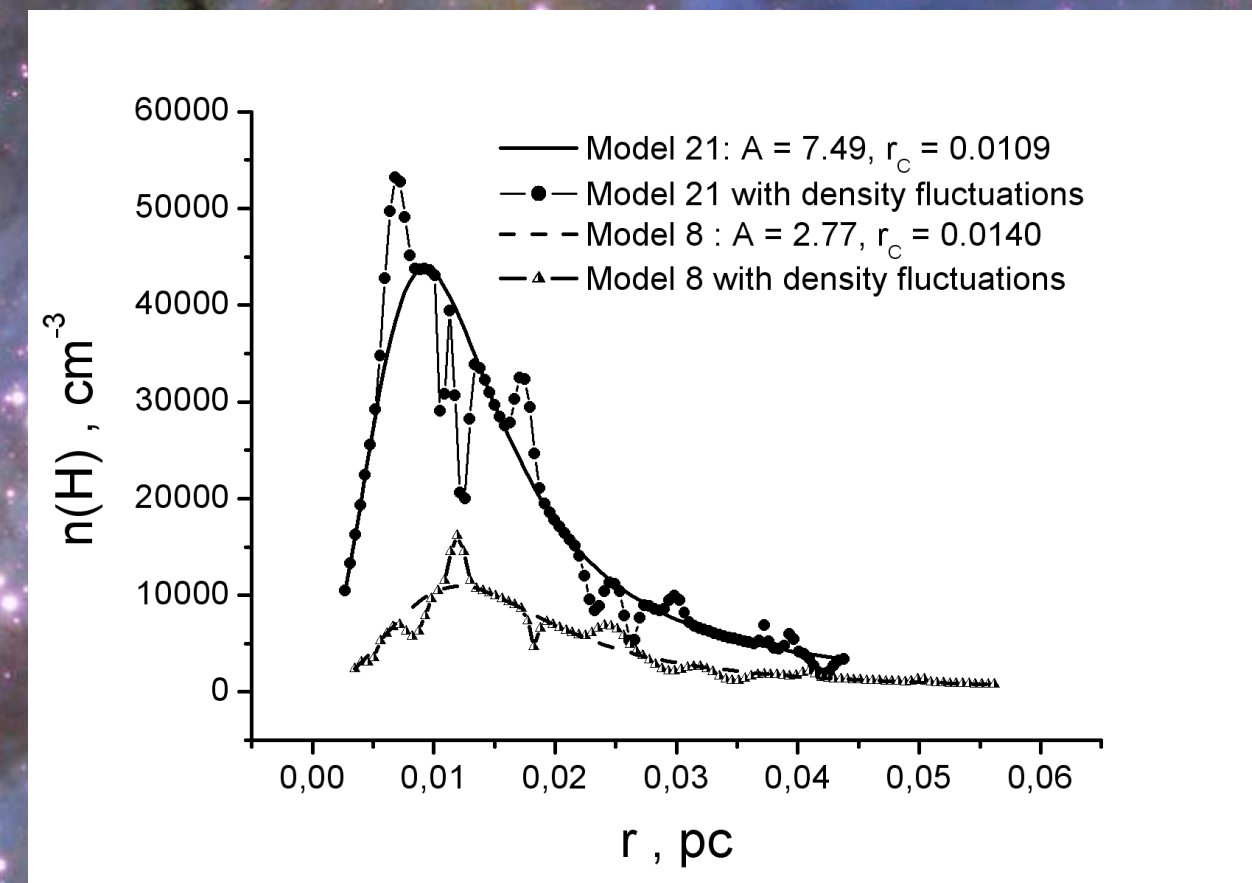
To allow for various types of gas density inhomogeneity in the PNe envelopes, we considered two types inhomogeneities of nebular gas density (Fig.1). Type I inhomogeneity (or macrofluctuation) corresponds to the radial distribution of gas density that was derived in [5] and was specified by the following empirical relationship:

$$n(r) = \frac{x^2(1+3e^{-1.2x})}{(x^2-1)^2 + 0.36r_c^0.43x^2r_c^2} A \quad (1)$$

where $x=r/r_c$ and $r_c=v_{exp}t$. Here r is the distance from the central star to a given point in the nebula, $n(r)$ is the gas density at this point, v_{exp} is the average expansion velocity of the envelope, and t is the envelope age (the values of r and r_c in (1) are given in parsecs). The parameter A describes the outflow of stellar material during the detachment of the nebular envelope [6]. The parameter A for every model was selected in order to value $n(r)$ from (1) and n_e obtained from ionization balance were equivalent. For most PNe the values of A are into the interval from 0.8 to 8.0, which corresponds to mass-lost rates of $(0.5 - 1.8)10^{-5} M_{\odot}/\text{year}$ at a velocity v_{exp} of about 15 km/s.

To take into account microfluctuations of the gas density (type II inhomogeneity) we developed code that superimposed inhomogeneities on the distribution (1) using a standard random-number generator. The input parameters were: (1) the parameters of the PN envelope: r_c and A [see (1)], and the inner and outer radii of the envelope r_{in} and r_{out} ($r_{in}=r_c/3$, $r_{out}=3r_c$); (2) the parameters of the inhomogeneities: n_{min} and n_{max} are the minimum and maximum numbers of fluctuations ($5 \leq 15$), d_{min} and d_{max} are the minimum and maximum sizes of the fluctuations in percent relative to the envelope radius $r=r_{out}-r_{in}$ (0.5 - 5%), ρ_{min} and ρ_{max} are the minimum and maximum deviations of the density of an inhomogeneity from the main distribution (5 - 30%), and the magnitudes of the fluctuations themselves (to 20%).

Fig.1. Radial distribution of the gas density in the envelopes of two PNe models.



For HII regions the free parameters were: the SED obtained for HII regions in BCDG by our method [7] from high-quality observations [8-10] of these objects (the method uses stellar atmosphere models of O-B stars [11-12]); the nebular gas filling factor (from 0.001 to 1); the relative abundance of heavy elements; the concentration of hydrogen atoms n_H .

In result we calculated 540 PNe PhMs and 270 HII regions PhMs. Integral spectra of these models were considered as "observed", and then they were analyzed by the standard method of nebular gas diagnostics using code DIAGN [13] with atomic data that correspond to the CLOUDY94 code data. We considered different dependences which allowed to determine the chemical composition as $\log(A/H) = \log(A^+/H^+) - f(x)$ (see method [5]). Here X^{k+l}/X^{m+k} corresponds to $\text{He}^{++}/\text{He}^+$, O^{++}/O^+ , S^{++}/S^+ or $\text{Ar}^{2+}/\text{Ar}^+$ and $x = \log(X^{k+l}/X^{m+k})$. All these correlations were approximated by polynomial function

$$f(x) = \sum_{n=0}^3 C_n x^n \quad (2)$$

where C_n are the polynomial coefficients. These expressions were tested for the purpose of reproduction of chemical composition given in corresponding PhMs and the accuracy was higher than 10% for best ICF expressions of PNe and HII regions in BCDG.

Obtained new analytical expressions for ICFs (see Tab.1 and Tab.2) were used for chemical composition determination of nebular gas in galactical PNe and in HII regions in BCDG. We have used PN spectra from different papers published previously (1976 - 1996 yr., see data on the ftp://astro.franco.lviv.ua/PN/Chem_CompPN2004) and HII regions spectra [8-10]. For PNe the abundances of He, N, O, Ne, S and Ar for 193 objects are determined and for HII regions in BCDG the corresponding data for 41 objects are determined.

The He/H abundance is determined using new emissivities from Benjamin et al. [14] and method of Olive & Skillman [15] for two types of the nebular objects. Analysis of the formulas for helium abundance indicated that they are not entirely exact, so we adopted ICF(He) = 1 when determining the helium abundance; i.e., $\text{He}/\text{H} = \text{He}^+/\text{H}^+ + \text{He}^{++}/\text{H}^+$.

We also analyzed possible gradients of the elements abundances with distance from the Galactic center for type II of PNe. The abundance gradients for each element studied, $d(\log(A/H))/dR$, in kpc^{-1} are:

- $(\text{He}/\text{H})^* = -0.0124 \pm 8.97 \cdot 10^{-6}$ ($n = 16$);
- $(\text{He}/\text{H})^{**} = -0.0082 \pm 2.86 \cdot 10^{-6}$ ($n = 60$);
- $\text{O}/\text{H}(I) = -0.0252 \pm 0.0118$ ($n = 65$);
- $\text{O}/\text{H}(II) = -0.0180 \pm 0.0183$ ($n = 61$);
- $\text{N}/\text{H}(I) = -0.0287 \pm 0.0179$ ($n = 66$);
- $\text{N}/\text{H}(II) = -0.0215 \pm 0.0201$ ($n = 61$);
- $\text{Ne}/\text{H}(I) = -0.0330 \pm 0.0131$ ($n = 59$);
- $\text{Ne}/\text{H}(II) = -0.0322 \pm 0.0312$ ($n = 16$);
- $\text{S}/\text{H}(I) = -0.0255 \pm 0.0139$ ($n = 62$);
- $\text{S}/\text{H}(II) = -0.0234 \pm 0.0150$ ($n = 59$);
- $\text{Ar}/\text{H}(I) = -0.0247 \pm 0.0156$ ($n = 55$);
- $\text{Ar}/\text{H}(II) = -0.0280 \pm 0.0169$ ($n = 48$).

While deriving the helium-abundance gradients, we used the data for PNe with 4 HeI lines ($(\text{He}/\text{H})^*$) and the average values $\langle \text{He}/\text{H} \rangle$ ($(\text{He}/\text{H})^{**}$) taking into account the corresponding errors. Data for the two types of inhomogeneity are presented ($A/H(I)$ and $A/H(II)$). The number of objects (n) used to find each gradient is given in parentheses. We adopted the PNe distances R from [16]. Our calculations cover Galactocentric distances $R = 2-15 \text{ kpc}$.

Although the distance scale adopted strongly affects the values of the gradients, our helium-abundance gradients coincide with the data of [17], and the gradients of other elements coincide with the data of [18] within the errors.

Table 1. New ICFs for PNe.

ICFs for type I (F) and type II (FF) inhomogeneity in the gas density distribution.										
N	A ^{+/H⁺}	X ^{m+k} /X ^{n+k}	Polynomial coefficients				ϵ	(A/H) _{obs}	(A/H) _{mod}	SD
He/H: $1.2(x \in [-3.012, -0.173])$										
F1	He ⁺	He ²⁺ /He ⁺	-0.23870	-0.60140	-0.33475	-0.05832	0.91	1.011		
F2	He ²⁺	He ²⁺ /He ²⁺	-0.23870	-0.39860	-0.33475	-0.05832	0.99	1.011		
O/H: $3(x \in [-0.848, 1.445]); 3(x \in [-0.601, 1.111]); 3(x \in [-1.538, -0.278])$										
F3	O ⁺	O ²⁺ /O ⁺	-0.27782	-0.62239	-0.34683	-0.05832	0.96	1.149		
F4	O ²⁺	O ²⁺ /O ²⁺	-0.27782	-0.40161	-0.34683	-0.05832	0.93	1.008		
F5	O ⁺	S ²⁺ /S ⁺	-1.36980	-2.26755	-1.44714	-0.32455	0.84	1.041		
F6	N ⁺	O ²⁺ /O ⁺	-0.27782	-0.62239	-0.34683	-0.05832	0.96	1.149		
F7	N ⁺	S ²⁺ /S ⁺	-1.36980	-2.26755	-1.44714	-0.32455	0.88	1.189		
F8	N ⁺	Ar ²⁺ /Ar ⁺	-1.30059	-2.17432	-1.43771	-0.34048	0.84	0.870		
Ne/H: $9(x \in [-0.708, 1.502]); 10(x \in [-2.042, 0.101])$										
F9	Ne ⁺	O ²⁺ /O ⁺	-0.06150	-0.08428	-0.21927	-0.06389	0.43	1.024		
F10	Ne ⁺	Ar ²⁺ /Ar ⁺	-0.32702	-0.51322	-0.22932	-0.06919	0.49	1.016		
S/H: $11(x \in [-0.821, 1.407]); 12(x \in [-0.842, 1.243]); 13(x \in [-0.598, 1.093]); 14(x \in [-2.077, 0.121])$										
F11	S ⁺	O ²⁺ /O ⁺	-0.33362	-0.62060	-0.26100	-0.07336	0.94	1.021		
F12	S ²⁺	O ²⁺ /O ⁺	-0.17925	-0.03041	-0.36505	-0.03666	0.78	1.007		
F13	S ⁺	S ²⁺ /S ⁺	-0.20142	-0.86441	-0.72479	-0.11284	0.94	1.015		
F14	S ⁺	Ar ²⁺ /Ar ⁺	-1.37832	-2.40162	-1.76205	-0.45066	0.79	1.093		
Ar/H: $15(x \in [-0.821, -1.424]); 16(x \in [-0.864, 1.445]); 17, 18(x \in [-2.060, 0.120])$										
F15	Ar ⁺	O ²⁺ /O ⁺	-0.07643	-0.22497	-0.23215	-0.03283	0.76	1.017		
F16	Ar ⁺	O ²⁺ /O ⁺	-0.58822	1.05332	-0.59124	-0.03053	0.88	1.050		
F17	Ar ⁺	Ar ²⁺ /Ar ⁺	-0.55070	-1.00470	-0.63547	-0.13461	0.78	1.015		
F18	Ar ⁺	Ar ²⁺ /Ar ²⁺	-0.55070	-0.04471	-0.63547	-0.13461	0.95	1.015		
He/H: $1(x \in [-3.496, 0.178]); 2(x \in [-3.223, -0.050])$										
FF1	He ⁺	He ²⁺ /He ⁺	-0.22559	-0.53991	-0.26682	-0.04109	0.74	1.011		
FF2	He ²⁺	He ²⁺ /He ²⁺	-0.13271	0.77099	-0.04971	-0.04971	0.99	1.016		
O/H: $3(x \in [-0.236, 1.095]); 6(x \in [-2.081, -0.177]); 4(x \in [-0.842, 1.315]); 5(x \in [-0.351, 0.728])$										
FF3	O ⁺	O ²⁺ /O ⁺	-0.28347	-0.60137	-0.41236	-0.06389	0.89	1.033		
FF4	O ²⁺	O ²⁺ /O ⁺	-0.29168	0.46012	-0.39720	-0.07055	0.94	1.016		
FF5	O ²⁺	S ²⁺ /S ⁺	-0.38583	0.78229	-0.68946	-0.13053	0.67	1.027		
FF6	O ⁺	Ar ²⁺ /Ar ⁺	-1.30051	-2.19380	-1.37547	-0.30467	0.84	1.051		
N/H: $7(x \in [-0.794, 1.413]); 8(x \in [-0.569, 0.668]); 9(x \in [-2.081, -0.052])$										
FF7	N ⁺	O ²⁺ /O ⁺	-0.27858	-0.62863	-0.34379	-0.06389	0.96	1.314		
FF8	N ⁺	S ²⁺ /S ⁺	-1.86448	-0.68632	-0.76086	-0.06389	0.87	1.326		
FF9	N ⁺	Ar ²⁺ /Ar ⁺	-1.28947	-2.09108	-1.34620	-0.31297	0.84	1.325		
Ne/H: $10(x \in [-2.0819, -0.187])$										
FF10	Ne ⁺	Ar ²⁺ /Ar ⁺	-0.32251	-0.49150	-0.19020	-0.06389	0.84	1.025		
S/H: $11(x \in [-0.769, 1.340]); 12(x \in [-0.601, 1.340]); 13(x \in [-0.351, 1.095]); 14(x \in [-2.050, -0.021]); 15(x \in [-1.155, -0.082])$										
FF11	S ⁺	O ²⁺ /O ⁺	-0.32238	-0.65139	-0.32790	-0.06389	0.93	1.031		
FF12	S ²⁺	O ²⁺ /O ⁺	-0.18345	-0.03747	-0.31307	-0.00846	0.76	1.014		
FF13	S ⁺	S ²⁺ /S ⁺	-0.19761	-0.85697	-0.76119	-0.12733	0.95	1.012		
FF14	S ⁺	Ar ²⁺ /Ar ⁺	-1.36910	-2.31242	-1.05119	-0.41463	0.79	1.095		
FF15	S ²⁺	Ar ²⁺ /Ar ²⁺	-0.58707	-1.06149	-0.83329	-0.19345	0.79	1.003		
Ar/H: $16(x \in [-0.794, 1.196]); 18(x \in [-2.081, 0.062]); 17(x \in [-0.754, 0.621]); 19(x \in [-2.092, -0.167])$										
FF16	Ar ⁺	O ²⁺ /O ⁺	-0.06961	-0.22044	-0.20368	-0.06389	0.74	1.020		
FF17	Ar ⁺	O ²⁺ /O ⁺	-0.98865	1.05557	-0.57037	-0.06337	0.88	1.049		
FF18	Ar ⁺	Ar ²⁺ /Ar ⁺	-0.55086	-1.00056	-0.62990	-0.13395	0.78	1.012		
FF19	Ar ⁺	Ar ²⁺ /Ar ²⁺	-0.55086	-0.68722	-0.62990	-0.13395	0.96	1.018		

Table 2. New ICFs for HII regions.

A/H = $10^{10} (A^{++}/H^{++}) - f(x)$, $f(x) = \sum_{n=0}^3 C_n x^n$												
N	A/H	A ^{+/H⁺}	C ₀	C ₁	C ₂	C ₃	C ₄	C ₅	C ₆	C ₇	SD	
x = $\log(\text{He}^{++}/\text{He}^+)$												
G1*	He/H	He ²⁺ /H ⁺	1043.9	2950.1	3318.2	1868.5	618.06	57.489	0	0	0.02	
x = $\log(\text{O}^{++}/\text{O}^+)$												
G2	O/H	O ²⁺ /H ⁺	-1.232	-0.470	-0.065	0.023	0	0	0	0	0.14	
G3*	O/H	O ²⁺ /H ⁺	-0.279	-0.432	-0.258	0.014	0.008	0	0	0	0.08	
G4*	O/H	O ²⁺ /H ⁺	-0.279	-0.279	-0.258	0.014	0.008	0	0	0	0.08	
x = $\log(\text{N}^{++}/\text{N}^+)$												
G5	N/H	N ²⁺ /H ⁺	-1.673	-1.008	-0.292	0.068	0.081	0	0	0	0.18	
G6*	N/H	N ²⁺ /H ⁺	-0.367	-0.489	-0.242	0.018	0.008	0	0	0	0.09	
G7*	Ne/H	Ne ²⁺ /H ⁺	-0.210	-0.459	-0.286	0.007	0.022	0	0	0	0.14	
G8	S/H	S ²⁺ /H ⁺	-0.547	-0.563	-0.131	0.015	0	0	0	0	0.13	
x = $\log(\text{Ar}^{2+}/\text{Ar}^+)$												
G9*	S/H	S ²⁺ /H ⁺	-0.167	0.062	0.014	0.158	-0.231	-0.05	0.07	0.006	-0.007	0.12
G10	Ar/H	Ar ²⁺ /H ⁺	-0.998	0.092	-0.117	0.001	-0.003	-0.008	0	0	0.07	
G11	Ar/H	Ar ²⁺ /H ⁺	-1.413	1.056	-0.258	-0.077	0.09	-0.009	-0.005	0	0.07	
x = $\log(\text{S}^{++}/\text{S}^+)$												
G12	He/H	He ²⁺ /H ⁺	0.043	0.017	0.013	0.015	0	-0.231	-0.05	0	0.03	
G13	O/H	O ²⁺ /H ⁺	-0.904	-0.893	-1.087	3.226	5.31	-22.53	20.58	-5.796	0.20	
G14*	O/H	O ²⁺ /H ⁺	-0.075	0.091	0.759	-0.817	-2.814	0.376	0.047	-0.467	0.29	
G15*	O/H	O ²⁺ /H ⁺	-0.743	0.885	-0.055	-0.031	-0.058	0	0	0	0.18	
x = $\log(\text{N}^{++}/\text{N}^+)$												